scientific reports

Check for updates

OPEN

A crack templated copper network film as a transparent conductive film and its application in organic light-emitting diode

Ping Liu[1]✉, Bing Huang[1,2], Lei Peng[2], Liming Liu[1], Qingguo Gao[1] & Yuehui Wang[1]

In this paper, a highly transparent, low sheet resistance copper network film fabricated by a crack template, which made by drying an acrylic based colloidal dispersion. The fabricated copper network film shows excellent optoelectronic performances with low sheet resistance of 13.4 Ω/sq and high optical transmittance of 93% [excluding Polyethylene terephthalate (PET) substrate] at 550 nm. What's more, the surface root mean square of the copper network film is about 4 nm, and the figure of merit is about 380. It's comparable to that of conventional indium tin oxide thin film. The repeated bending cycle test and adhesive test results confirm the reliability of the copper network film. As a transparent conductive film, the copper network film was used as an anode to prepare organic light-emitting diode (OLED). The experiment results show that the threshold voltage of the OLED is less than 5 V and the maximum luminance is 1587 cd/m^2.

Organic light-emitting diode (OLED) has attracted more and more attention, due to the characteristics of spontaneous light, ultra-thin, high contrast, low power consumption and simple structure. One of the important components in OLED is transparent conductive film (TCF). Indium tin oxide (ITO) thin films are usually used as the anodes for Organic light-emitting diodes (OLEDs). The ITO thin films don't meet the requirement of flexible equipment due to the characteristic of fragility, high cost and complex preparation process. In addition, The ITO thin films are easy to crack under bending, which leads to degradation of device performance[1]. Besides, The ITO thin films have significant light reflection characteristics[2]. Bending and impact resistance are the basic requirements of flexible equipment. Although there are some ITO films prepared on Polyethylene terephthalate (PET) substrate that can be used for flexible optoelectronic devices, their performances are lower than those ITO films prepared on some rigid substrates. Some researchers have started looking for alternatives of ITO, such as metal thin films. Recently, various substitutes have been developed. These transparent conductive films (TCFs) can be mainly divide into three categories. Carbon-based TCFs (graphene[3], carbon nanotubes (CNTs)[4]); metal based TCFs (metallic nanowires[5,6] and metallic network[7–9]) and hybrid TCFs[10–12].

Complete and defect-free graphene has high carrier mobility and high transmittance. However, the interlayer contact resistance is larger than ITO, and if you want to produce defect-free graphene, the high cost of preparation has to be considered [13]. CNTs have excellent photoelectric properties, thermal properties and mechanical stability. Carbon nanotube (CNT) was first discovered by Iijima[14] in 1991. However, it's difficult to control the length of CNTs and uniformity of diameter. Metallic nanowires can be easily synthesized by solution methods, such as hydrothermal method and polyol method, which is low cost and high efficiency[15]. Metallic nanowires, especially silver nanowires, have good mechanical flexibility and better trade-off between transmittance and electrical conductivity. Amit Kumar and co-workers systematically elaborate an abundant of approaches to forming silver nanowire for fabricating transparent conducting electrodes[16]. A host of metal-based TCFs have been applied in solar cells , biological devices and flexible touchscreen panels and displays[9,12]. It has been proved as an alternative to ITO[17,18] Hybrid TCFs of Carbon-based materials, metals and conductive polymers can effectively utilize the advantage of a single material and complement the shortcomings of a single material[19,20]. Cu-transparent conductive oxides show a broad work function and work as anode or cathode electrodes in organic light-emitting diodes (LEDs) without hole injection layer[21]. Meanwhile, hybrid transparent electrodes can improve charge injection and obtain better current density[22]. Thus, the hybrid TCFs with suitable energy-level alignments can improve

[1]College of Electron and Information Engineering, University of Electronic Science and Technology of China Zhongshan Institute, Zhongshan 528402, China. [2]School of Physics, University of Electronic Science and Technology of China, Chengdu 610054, China. ✉email: liuping49@126.com

Figure 1. Schematic illustration for preparing copper network films. (**a**) acrylic based crack template; (**b**) deposition of copper on a crack template; (**c**) lift-off the template.

the photoelectric performance and thermochemical stability[23]. As metallic network film, the trade-off between transmittance and conductivity is also better than ITO, what's more, it has better mechanical flexibility than ITO. Compared with metallic nanowires, there is no need to consider the influence of lap resistance. In addition, the geometry of metallic network film can be manipulated to submicron scale. Which is invisible to human eyes. This characteristic is vital in transparent electronic devices. At the same time, TCFs prepared by metallic network film is superior than ITO has been proved through theory. Yi Cui of Stanford University had testified that the transmittance and sheet resistance are better than ITO by electromagnetic simulation[24].

The fabrication of metallic network TCFs are as follows, electrospinning[25], photon sintering [26–28] lithography[29–31], additive manufacturing[32–34], ink-jet printing[35], etc. Typically, the preparation of metallic network film is divided into three processes, patterning, metallization and transfer. Patterning means the production of microstructures or nanostructures. The most common patterning methods are photolithography and nanoimprint lithography. During photolithography, rotating a thin layer photoresist on the substrate, then, a mask with the pattern coated under UV light to cover the photoresist. The photoresist is chemically changed when exposed to UV light and a template with micro-nanostructure is obtained after developed.

Crack template is a new method for making transparent conductive metallic network film[36–42]. Compared with nanoimprint lithography or photolithography, the raw materials for Crack template are low cost, usually for acrylic acid or titanium dioxide. Moreover, the making process of crack template is simple, material resources are extensive. Through the crack template method, the metallic network TCFs can be fabricated in large area. Nevertheless, copper has low resistivity and abundant reserves. Compare with silver, there are 1000 times more copper than silver and the price of copper is much cheaper than sliver, almost 1/100 times, but the conductivity is only 6% lower than silver[43]. So, copper network films based on crack templates are expected to be used in low-cost organic devices. One of the basic challenges for preparing copper network films is to obtain high light transmittance maintaining low sheet resistance and low surface roughness.

We have explored the viability of cracks as a template for the preparation of metallic network film from acrylic acid. The fabricated copper network films show excellent optoelectronic performances with low sheet resistance of 13.4 Ω/sq and high optical transmittance of 93% (excluding PET substrate) at 550 nm. The copper network film was used as an anode of a flexible OLED. The threshold voltage of the OLED is less than 5 V and the maximum luminance is 1587 cd/m^2.

Experimental section

Preparation of copper network film. PET was treated by oxygen plasma, which can improve the hydrophilicity of PET. The higher the hydrophilicity of the substrate, the more conducive to the formation of microcracks. The acrylic was diluted with alcohol in a 3:2 volume ratio, and then filter twice through a vacuum filter. The process for preparation copper network films is shown schematically in Fig. 1. Firstly, a crack template was made by drying an acrylic based colloidal dispersion, which coated on PET. After cracking, these cracks are completely detached from the substrate. And then, basing on the template, the copper is deposited by vacuum evaporation. In the final step of lift-off, we use a syringe to drain tetrahydrofuran to flush the surface of the template. Propylene glycol methyl ether acetate (PGMEA) was used for ultrasound for 15 min. As shown in Fig. 2, highly interconnected cracks are obtained spontaneously.

Fabrication of flexible OLED based on copper network film. In this paper, we have prepared an OLED with a common structure by vacuum evaporation equipment. The structure of OLED as shown in Fig. 3. For OLED, the roughness of TCFs has a significant influence, excessive roughness may cause a short circuit. Therefore, copper network film fabricated at 2000 r/min was used as an anode, the surface root-mean-square (RMS) roughness is about 4 nm. PEDOT:PSS was used as the hole injection layer, *N*,*N*′-bis(1-naphthyl)-*N*,*N*′-diphenyl-1,1′-biphenyl-4,4′-diamine (NPB) was used as the hole transport layer, tris (8-hydroxyquinoline) aluminium (Alq_3) was used as the electron transport layer and the emitting layer, LiF was used as the electron injection layer, Al was used as the cathode. The device structure of the OLED and thickness of each layer is indicated in Fig. 3.

Result and discussion

Transmittance was measured with an ultraviolet–visible–near infrared photometer (UH4150, HITACHI) with an integrating sphere attached. Sheet resistance was measured using a four-point probe system (DMR-1C) and multimeter. Optical microscopy images were taken using Olympus BX51M. The characterization of copper network film was measured by AFM (BRUKER, Dimension Edge). Bending test was done using an ordinary pen, which diameter is 9 mm. The adhesion test was performed using a 3 M scotch tape to attach onto the copper network film and then peeled off, records the resistance every 10 times.

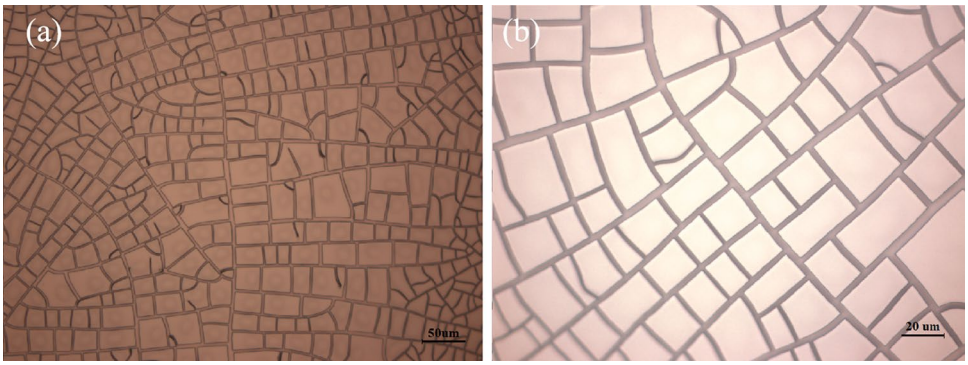

Figure 2. Optical microscope images of crack morphology in different magnification: (**a**) 200 times, (**b**) 500 times.

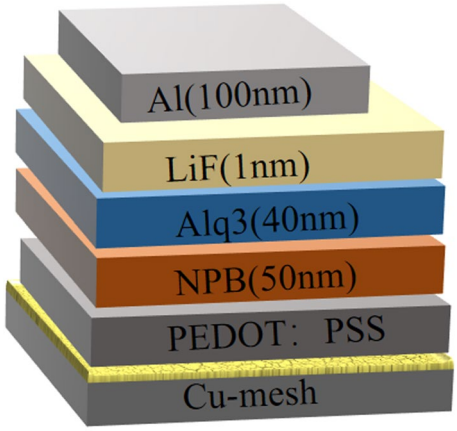

Figure 3. The device structure of the OLED.

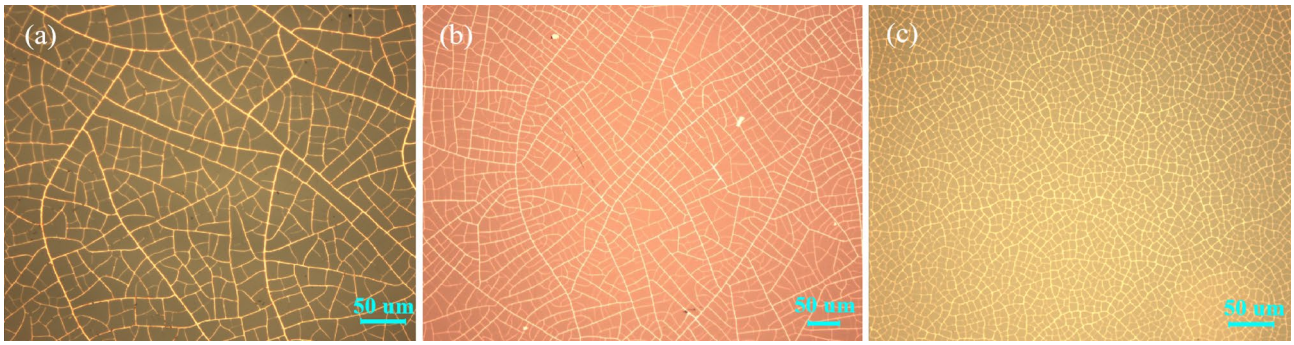

Figure 4. Optical microscope images of copper network films with different coating speeds: (**a**) 1500 r/min, (**b**) 2000 r/min, (**c**) 2400 r/min.

Microstructure of copper network film. Copper network films fabricated by crack template are shown in Fig. 4, where the inside scale is 50 μm. The density of copper network film is increasing with the increase of coating speed. However, when the coating speed exceeds a certain value, the copper wires started to crack slightly, which affects conductivity (see Fig. 4c). The template was made of acrylic resin, which is rotated for 60 s by a spin coater and then dried at 100 °C on a constant temperature heating table for 1 h.

Sheet resistance and transmittance of copper network film. The spin coating speed affects the morphology of the crack template. If the speed is too slow, the width of crack will be too wide. If the speed is too fast, the interconnection of crack is very poor. The wider the crack, the more copper is deposited, which means that copper wires occupy more area, thus affecting the transmittance of the film. When the interconnection of crack is very poor, the conductivity of the film will be affected. Therefore, we chose an appropriate interval, in a

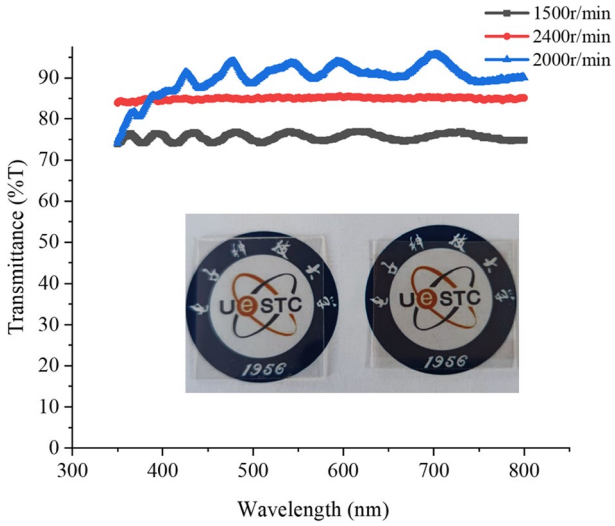

Figure 5. The transmittance of copper network films with different coating speed.

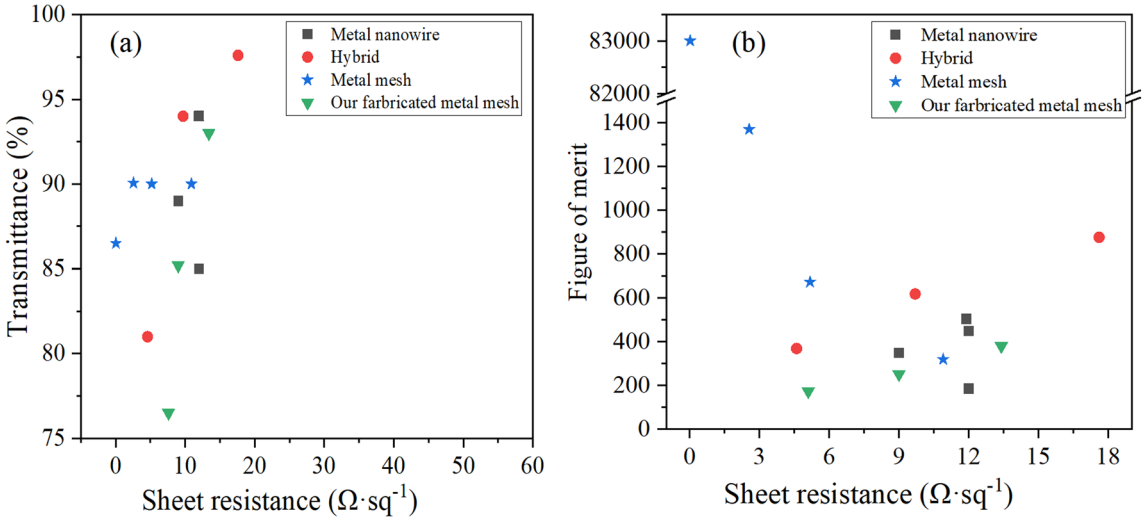

Figure 6. Performances of the flexible TCFs. (**a**) Transmittance versus sheet resistance data of the metallic network in comparison with previous studies (metallic wire[13,44–46], metallic network[9,25,33,47], hybrid [48–50]), (**b**) Comparison of the figure of merit values.

valid speed range, as coating speed increases, the thickness of the template decreases and the width of the cracks becomes finer. The transmittance of our copper network TCFs are shown in Fig. 5. These templates were made by three different coating speed. The transmittance of a copper network TCF was 76.5% at 550 nm, whose template was coated at 1500 r/min for 60 s. The sheet resistance of the copper network TCF is 3.4 Ω/sq and the surface RMS roughness is 33.2 nm. It's worth noting that the transmittance of all copper network films in this paper refers to the transmittance excluding PET substrate. Based on the template fabricated at 2000 r/min, the copper network TCF with transmittance of 93% and sheet resistance of 13.4 Ω/sq were obtained. The RMS roughness of the copper network TCF is as low as 4 nm. The built-in figure is a comparison of transmittance between a clean PET substrate (see the left figure) with a copper network TCF with transmittance of 93% (see the right figure). As you can see that the word UESTC under the TCFs is still can be seen clearly. Based on the template fabricated at 2400 r/min, the transmittance of the copper network TCF is 85.2% and sheet resistance is 7.2 Ω/sq.

Figure 6 shows the performances comparation of the flexible copper network TCFs. Transmittance at the wavelength of 550 nm and the sheet resistance values are plotted, in order to compare with the result of previous studies (metallic nanowire[13,44–46] metallic network[9,25,33,47], hybrid[48–50]). Figure of merit (FoM) were calculated, the calculation formula is as follows[51]

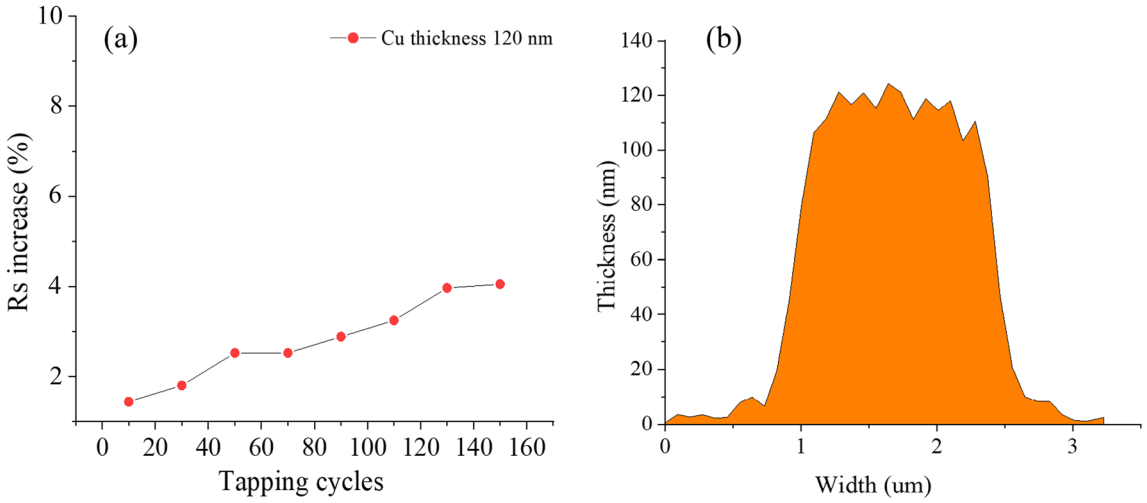

Figure 7. (**a**) Variation graph of sheet resistance during the adhesive tape test and. (**b**) AFM diagram of copper wire thickness.

$$\mathrm{FoM} = \frac{\delta_{\mathrm{dc}}}{\delta_{\mathrm{opt}}} = \frac{188.5}{\mathrm{R_s}\left(\frac{1}{\sqrt{\mathrm{T}}} - 1\right)}, \tag{1}$$

where δ_{dc} is the electrical conductance and δ_{opt} is the optical conductance[51], R_s means sheet resistance and T denotes transmittance. As shown in Fig. 6a, the sheet resistance of the TCFs prepared by us is well, while the transmittance of TCFs changes greatly, which is still related to the cleaning operation.

Hybrid type and metallic network type TCFs demonstrated outstanding performance in comparison with metallic nanowire based TCFs. As shown in Fig. 6b, the FoM of our TCFs is about 380, compared with commercial ITO which FoM is about 200, it has certain application prospect.

Mechanical properties of copper network film. For bulk materials, ρ is usually used to measure the conductivity of the material. The measurement of conductivity involves the thickness t of the material, but the thickness of TCFs is usually nonuniform, the concept of square resistance is introduced to measure the conductivity of TCFs. As shows in the following formula.

$$\mathrm{R_s} = \frac{\rho}{\mathrm{t}}, \tag{2}$$

According to Formula (2), ρ is an intrinsic property of a material, the sheet resistance decreases with the increase of thickness, and the increase of the thickness will bring the decrease of the transmittance. This explains why there is a trade-off between transmittance and conductivity. Due to the use of four-probe test will cause irreversible defects on the film surface, which will seriously affect the subsequent preparation of OLED devices. The sheet resistance is determined by

$$\mathrm{R} = \mathrm{R_s}\frac{\mathrm{L}}{\mathrm{W}}, \tag{3}$$

where R is the resistance measured by a multimeter, R_s is the sheet resistance of TCFs, L is the length of the TCFs between the two polos, and W is the width of the TCFs. By Formula (3), we could calculate the final sheet resistance of the film. In our test, the length of the TCFs between the poles is 20 mm, and the width of the TCFs is 30 mm.

Mechanical stability of a copper network TCF were tested by 3 M adhesive tape and cyclic bending[38]. The tapping test was conducted to evaluate the adhesion between the copper network film and PET substrates. Figure 7a shows the variation curve of square resistance with adhesive tape test times. After 160 cycles, the sheet resistance of the TCFs changes slightly, about 3%. Indicating that the copper network film has good adhesion. Figure 7b shows the thickness of the copper network wire and the thickness is about 120 nm.

As cyclic bending, we bend with the help of a common pen, which has a diameter of 9 mm as shown in the built-in diagram. We bent 600 times and measured the resistance every 100 times. The data obtained are shown in Table 1.

Figure 8 shows the result of cyclic bending test of a copper network TCF. During 500 times bends, our copper network TCF maintains low sheet resistance. When the bending times exceeds 500, the sheet resistance increases rapidly with the increase of bending times. After bending 600 times, the film shows obviously signs of bending, as shown in Fig. 9a. The network film at the crease of the TCFs was observed by optical microscope, see in Fig. 9b. There are some fractures of copper network film at the crease. However, we found that the film still has conductivity, as shown in Fig. 9c, the conductivity of the film was tested with a multimeter and a light-emitting

Number of bending	Resistance	Sheet resistance	Rate of change of sheet resistance
0	5.1	7.65	0%
100	5.2	7.8	1.96%
200	5.3	7.95	1.92%
300	5.4	8.1	1.89%
400	5.6	8.4	3.70%
500	5.9	8.85	5.30%
600	27.2	40.8	361%

Table 1. Bending test data

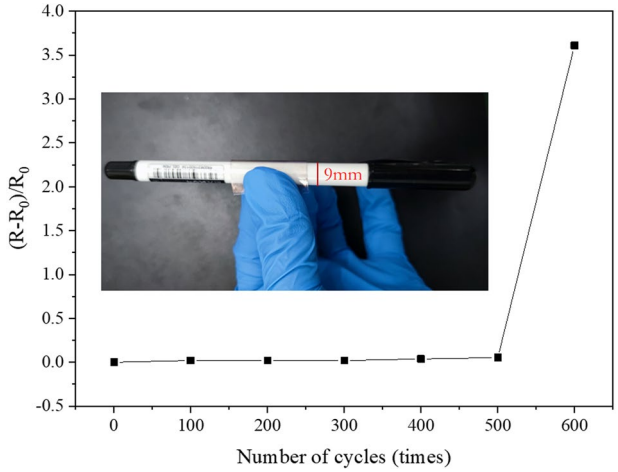

Figure 8. Bending test of the flexible transparent films.

diode. When the conductivity was measured again, it was found that the resistance of the film had changed from initial 5.1 Ω to 27.2 Ω, as shown in Fig. 9d.

Photoelectric performance of the flexible OLED based on copper network film. Keithley 2400 digital source meter and PR655 spectrometer system were used to test the performance of OLED. When the brightness reaches 1 cd/m^2 driven by the voltage, this voltage is called threshold voltage. The luminance of our OLED reaches 1.679 cd/m^2 at 5 V, that indicates the starting voltage of our device is below 5 V. Figure 10a shows a uniform light of OLED without specks, in addition, it's also bright under curved. It's worth noting that an excessive rate of evaporation will lead to a lack of compactness of the organic functional layer, which leads to nonuniform brightness. The evaporation rate of organic layer in this experiment is 0.2 A/s. Figure 10b, c show the current density–voltage characteristic and brightness-voltage characteristic of the OLED, respectively. The maximum luminance of the OLED was 1587 cd/m^2. As the voltage increases, the current density increases, so does the brightness. Beyond a certain voltage, the current rise sharply. While the brightness increases rapidly along with the current density increases. However, as the voltage continues to increase, the OLED performance is declining rapidly. The possible reason for this phenomenon is that as the voltage continues to increase, the current density increases, resulting in increasing of joule heat, and then leads to an increase in temperature. The rise in temperature destroys the organic functional layer, so that it reduces the probability of effective recombination of excitons. Thus, the performance of the OLED is affected. Figure 10d is the current density in log scale versus voltage for the OLED. Figure 10e demonstrates current efficiency and power efficiency of the OLED.

Conclusion

We demonstrated a facile fabrication strategy for copper network TCFs, based on a crack template. This method does not need complex stripping and transfer processes, what's more, the crack template is universal for any type of metallic or substrate material. The copper network film exhibited a high transmittance of about 93% at 550 nm with sheet resistance of 13.4 Ω/sq. The figure of merit is about 380, which comparable to ITO. Another copper network TCFs produced by this method exhibited transmittance 76.5% with sheet resistance of 3.4 Ω/sq, at a copper film thickness of 120 nm. The mechanical properties network film was also investigated based on these copper network TCFs. During 500 times bends, the copper network TCFs maintain a low sheet resistance. In addition, the demonstration of flexible OLED prepared using the TCFs suggests its promising applicability. The threshold voltage of the OLED is less than 5 V and the maximum luminance is 1587 cd/m^2. The crack template

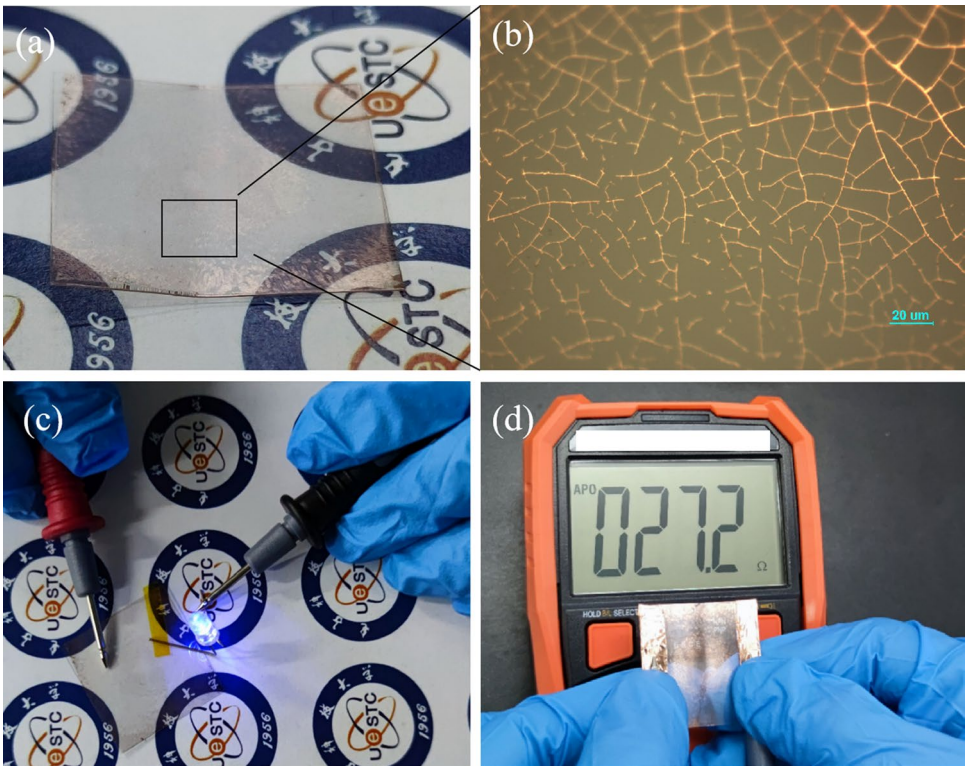

Figure 9. Characterization of TCFs after bending test, (**a**) TCFs after bending, (**b**) optical microscope at the crease, (**c**) schematic diagram of conductivity of TCFs, (**d**) resistance of TCFs after bending.

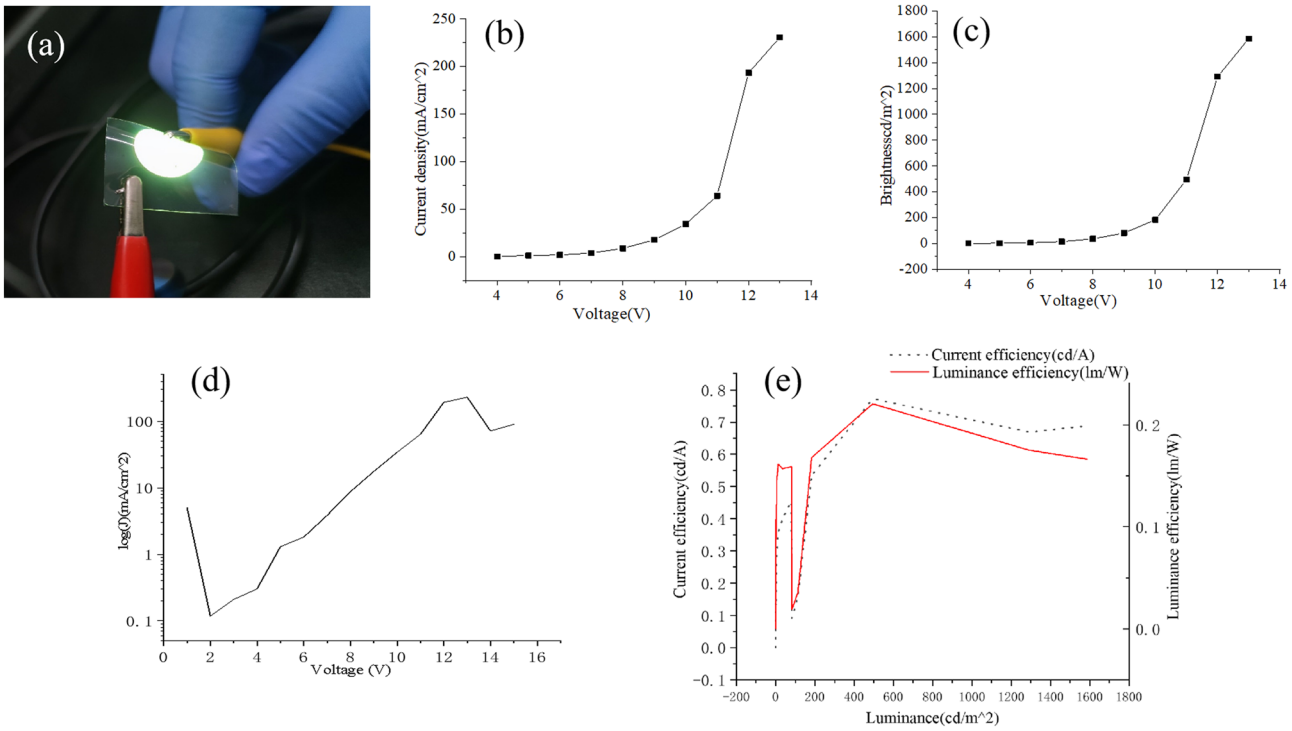

Figure 10. Photoelectric performance of the flexible OLED based on copper network film. (**a**) Luminescence diagram of flexible OLED at 10 V. (**b**) Current density–voltage characteristic of OLED device. (**c**) Brightness-voltage characteristic of the OLED. (**d**) Current density in log scale versus voltage. (**e**) Current efficiency and power efficiency of the OLED.

method for preparing copper grid TCFs may provide an alternative route for low-cost and large-area production of a variety of other device components, such as organic solar cells, transparent heater and supercapacitor.

Data availability

All data generated or analysed during this study are included in this published article.

Received: 27 June 2022; Accepted: 18 November 2022
Published online: 28 November 2022

References

1. Lee, H. B., Jin, W. Y., Ovhal, M. M., Kumar, N. & Kang, J. W. Flexible transparent conducting electrodes based on metal meshes for organic optoelectronic device applications: A review. *J. Mater. Chem. C* **7**, 1087–1110 (2019).
2. Brutting, W., Frischeisen, J., Schmidt, T. D., Scholz, B. J. & Mayr, C. Device efficiency of organic light-emitting diodes: Progress by improved light outcoupling. *Physica Status Solidi A Appl. Mater. Sci* **210**, 44–65 (2013).
3. Backes, C., Abdelkader, A. M., Alonso, C., Andrieux-Ledier, A. & Garcia-Hernandez, M. Production and processing of graphene and related materials. *2D Materials* **7**, 022001 (2020).
4. Zhu, Z. R. *et al.* Highly transparent, low sheet resistance and stable Tannic acid modified-SWCNT/AgNW double-layer conductive network for organic light emitting diodes. *Nanotechnology* **32**, 015708 (2021).
5. Wang, Y. X. *et al.* Flexible organic light-emitting devices with copper nanowire composite transparent conductive electrode. *J. Mater. Sci.* **54**, 2343–2350 (2019).
6. Wang, Y., Liu, P., Zeng, B., Liu, L. & Yang, J. Facile synthesis of ultralong and thin copper nanowires and its application to high-performance flexible transparent conductive electrodes. *Nanoscale Res. Lett.* **13**, 1–10 (2018).
7. Han, S. *et al.* High-performance solution-processable flexible and transparent conducting electrodes with embedded Cu mesh. *J. Mater. Chem. C* **6**, 4389–4395 (2018).
8. Chang, L. *et al.* Ionogel/copper grid composites for high-performance, ultra-stable flexible transparent electrodes. *ACS Appl. Mater. Interfaces* **10**, 29010–29018 (2018).
9. Nguyen, V. H. *et al.* Advances in flexible metallic transparent electrodes. *Small* **18**, 2106006 (2022).
10. Liu, P. *et al.* A new structure of flexible OLED with copper nanowire anode and graphere oxide/pedot: PSS anode buffer layer. *Surf. Rev. Lett.* **27**, 1950171 (2020).
11. Wang, S. *et al.* Chemical and thermal robust tri-layer rGO/Ag NWs/GO composite film for wearable heaters. *Compos. Sci. Technol.* **174**, 76–83 (2019).
12. Yang, Y. R., Wang, Y. & Song, Y. L. Flexible transparent electrodes based on metallic micro-nano architectures for perovskite solar cells. *J. Mater. Chem. C* **10**, 2349–2363 (2021).
13. Azani, M. R., Hassanpour, A. & Torres, T. Benefits, problems, and solutions of silver nanowire transparent conductive electrodes in indium tin oxide (ITO)-free flexible solar cells. *Adv. Energy Mater.* **10**, 2002536 (2020).
14. Iijima, S. helical microtubules of graphitic carbon. *Nature* **354**, 56–58 (1991).
15. Wang, Y. X., Liu, P., Zeng, B. Q., Liu, L. M. & Yang, J. J. Facile synthesis of ultralong and thin copper nanowires and its application to high-performance flexible transparent conductive electrodes. *Nanoscale Res. Lett.* **13**, 78 (2018).
16. Kumar, A., Shaikh, M. O. & Chuang, C. H. Silver nanowire synthesis and strategies for fabricating transparent conducting electrodes. *Nanomaterials* **11**, 693 (2021).
17. Li, X. S., Wang, Y. M., Yin, C. R. & Yin, Z. X. Copper nanowires in recent electronic applications: Progress and perspectives. *J. Mater. Chem. C* **8**, 849–872 (2020).
18. Nguyen, D. T. & Youn, H. Facile fabrication of highly conductive, ultrasmooth, and flexible silver nanowire electrode for organic optoelectronic devices. *ACS Appl. Mater. Interfaces.* **11**, 42469–42478 (2019).
19. Hwang, Y. *et al.* Ag-fiber/graphene hybrid electrodes for highly flexible and transparent optoelectronic devices. *Sci. Rep.* **10**, 5117 (2020).
20. Keum, C. *et al.* A substrateless, flexible, and water-resistant organic light-emitting diode. *Nat. Commun.* **11**, 6250 (2020).
21. Kang, D. Y. *et al.* Dopant-tunable ultrathin transparent conductive oxides for efficient energy conversion devices. *Nano Micro Lett* **13**, 445–459 (2021).
22. Jang, I. G. *et al.* Cavity-suppressing electrode integrated with multi-quantum well emitter: A universal approach toward high-performance blue TADF top emission OLED. *Nano Micro Lett.* **14**, 81–95 (2022).
23. Yang, J. J. *et al.* ITO electrode with a tunable work function for organic photovoltaic devices. *ACS Appl. Electron. Mater.* **4**, 4104–4112 (2022).
24. Lee, J. Y., Connor, S. T., Cui, Y. & Peumans, P. Solution-processed metal nanowire mesh transparent electrodes. *Nano Lett.* **8**, 689–692 (2008).
25. Singh, S. B., Hu, Y. B., Kshetri, T., Kim, N. H. & Lee, J. H. An embedded-PVA@Ag nanofiber network for ultra-smooth, high performance transparent conducting electrodes. *J. Mater. Chem. C* **5**, 4198–4205 (2017).
26. Jung, J. *et al.* Moire-Free imperceptible and flexible random metal grid electrodes with large figure-of-merit by photonic sintering control of copper nanoparticles. *ACS Appl. Mater. Interfaces* **11**, 15773–15780 (2019).
27. Song, S. & Cho, S. M. Transparent Metal-Mesh heater using Silver-coated copper nanoparticles sintered with intense pulsed light irradiation on PET substrate. *Korean J. Chem. Eng.* **38**, 1720–1726 (2021).
28. Chen, X. L. *et al.* Hybrid printing metal-mesh transparent conductive films with lower energy photonically sintered copper/tin ink. *Sci. Rep.* **7**, 13239 (2017).
29. Li, L. J. *et al.* Fabrication of flexible transparent electrode with enhanced conductivity from hierarchical metal grids. *ACS Appl. Mater. Interfaces* **9**, 39110–39115 (2017).
30. Yi, F. S. *et al.* Plasmonic ultrathin metal grid electrode induced optical outcoupling enhancement in flexible organic light-emitting device. *Org. Electron.* **87**, 105960 (2020).
31. Khan, A. *et al.* High-performance flexible transparent electrode with an embedded metal mesh fabricated by cost-effective solution process. *Small* **12**, 3021–3030 (2016).
32. Cui, Z. & Gao, Y. Hybrid printing of high resolution metal mesh as a transparent conductor for touch panels and OLED displays. *SID International Symposium: Digest of Technology Papers.* **46**, 398–400 (2015).
33. Chen, X. L. *et al.* Printable high-aspect ratio and high-resolution cu grid flexible transparent conductive film with figure of merit over 80 000. *Adv. Electron. Mater.* **5**, 1800991 (2019).
34. Wang, Z., Kang, Y., Zhao, S. C. & Zhu, J. Self-Limiting assembly approaches for nanoadditive manufacturing of electronic thin films and devices. *Adv. Mater.* **32**, 1806480 (2020).
35. Zhang, B., Lee, H. D. & Byun, D. Electrohydrodynamic jet printed 3d metallic grid: Toward high-performance transparent electrodes. *Adv. Eng. Mater.* **22**, 1901275 (2020).
36. Gupta, R. *et al.* Spray coating of crack templates for the fabrication of transparent conductors and heaters on flat and curved surfaces. *ACS Appl. Mater. Interfaces* **6**, 13688–13696 (2014).

37. Rao, K. D. M., Hunger, C., Gupta, R., Kulkarni, G. U. & Thelakkat, M. A cracked polymer templated metal network as a transparent conducting electrode for ITO-free organic solar cells. *Phys. Chem. Chem. Phys.* **16**, 15107–15110 (2014).
38. Zhu, C. T. *et al.* A cracked polymer templated Ag network for flexible transparent electrodes and heaters. *Mater. Res. Express* **5**, 066427 (2018).
39. Walia, S., Singh, A. K., Rao, V. S. G., Bose, S. & Kulkarni, G. U. Metal mesh-based transparent electrodes as high-performance EMI shields. *Bull. Mater. Sci.* **43**, 1–8 (2020).
40. Kiruthika, S. & Kulkarni, G. U. Energy efficient hydrogel based smart windows with low cost transparent conducting electrodes. *Sol. Energy Mater. Sol. Cells* **163**, 231–236 (2017).
41. Muzzillo, C. P., Reese, M. O. & Mansfield, L. M. Fundamentals of using cracked film lithography to pattern transparent conductive metal grids for photovoltaics. *Langmuir* **36**, 4630–4636 (2020).
42. Gedda, M., Das, D., Iyer, P. K. & Kulkarni, G. U. Work function tunable metal-mesh based transparent electrodes for fabricating indium-free organic light-emitting diodes. *Mater. Res. Express* **7**, 054005 (2020).
43. Kumar, D. V. R., Woo, K. & Moon, J. Promising wet chemical strategies to synthesize Cu nanowires for emerging electronic applications. *Nanoscale* **7**, 17195–17210 (2015).
44. Bai, S. C., Yang, H., Wang, H. F. & Guo, X. Z. Fabrication of water base silver nanowire conductive ink and large scale flexible transparent conductive film. *Rare Metal Mater. Eng.* **49**, 1282–1287 (2020).
45. Wang, S., Tian, Y. H., Wang, C. X. & Hang, C. J. Communication-AgNW networks enhanced by ni electroplating for flexible transparent electrodes. *J. Electrochem. Soc.* **165**, D328–D330 (2018).
46. Lee, J. *et al.* Very long Ag nanowire synthesis and its application in a highly transparent, conductive and flexible metal electrode touch panel. *Nanoscale* **4**, 6408–6414 (2012).
47. Yang, J., Bao, C. X., Zhu, K., Yu, T. & Xu, Q. Y. High-performance transparent conducting metal network electrodes for perovksite photodetectors. *ACS Appl. Mater. Interfaces* **10**, 1996–2003 (2018).
48. Ji, Y. X. *et al.* Ultraflexible and high-performance multilayer transparent electrode based on ZnO/Ag/CuSCN. *ACS Appl. Mater. Interfaces* **10**, 9571–9578 (2018).
49. Bai, S. C. *et al.* Solution processed fabrication of silver nanowire-MXene@PEDOT: PSS flexible transparent electrodes for flexible organic light-emitting diodes. *Compos. Part A Appl. Sci. Manuf.* **139**, 106088 (2020).
50. Gao, Y., Wang, W. C., Song, N. N., Gai, Y. Z. & Zhao, Y. P. Fabrication of highly flexible transparent conductive film with a sandwich-structure consisted of graphene/silver nanowire/graphene. *J. Mater. Sci. Mater. Electron.* **28**, 17031–17037 (2017).
51. Zhou, H. & Song, Y. Fabrication of silver mesh/grid and its applications in electronics. *ACS Appl. Mater. Interfaces* **13**, 3493–3511 (2021).

Author contributions

B.H. did the most experiments in this work, B.H. and P.L. drafted the manuscript, L.P. completed revision of the manuscript, P.L.made the research plan, Q.G.G., L.M.L. and Y.H.W. provided helpful guidance and suggestions. All the authors read and approved the final manuscript.

Funding

This work was supported by the National Natural Science Foundation of China (No. 62104033), the Key Scientific Research Project of the Department of Education of Guangdong Province (2021ZDZX1052, 2021GCZX005, and 2020KCXTD030), the Basic and Applied Basic Research Foundation of Guangdong Province (No. 2019A1515110752), and the Science and Technology Project Foundation of Zhongshan City (2022B2020 and 2022B2006).

Competing interests

The authors declare no competing interests.

Additional information

Correspondence and requests for materials should be addressed to P.L.

Reprints and permissions information is available at www.nature.com/reprints.

Publisher's note Springer Nature remains neutral with regard to jurisdictional claims in published maps and institutional affiliations.